

The three-dimensional Heisenberg spin glass under a weak random anisotropy.

V. Martin-Mayor^{1,2} and S. Perez-Gaviro^{3,2}

¹*Departamento de Física Teórica I, Facultad de Ciencias Físicas, Universidad Complutense, 28040 Madrid, Spain.*

²*Instituto de Biocomputación y Física de Sistemas Complejos (BIFI), Corona de Aragón 42, Zaragoza 50009, Spain.*

³*Dipartimento di Fisica, INFN and INFN, Università di Roma La Sapienza, Ple. A. Moro 2, 00185 Roma, Italy.*

(Dated: June 8, 2018)

We perform a finite size scaling study of the three-dimensional Heisenberg spin glass in the presence of weak random anisotropic interactions, up to sizes $L = 32$. Anisotropies have a major impact on the phase transition. The chiral-glass susceptibility does not diverge, due to a large anomalous dimension. It follows that the anisotropic spin-glass belongs to a Universality Class different from the isotropic model, which questions the applicability of the chirality scenario.

PACS numbers: 75.50.Lk 75.40.Mg. 64.60.F-, 05.50.+q,

I. INTRODUCTION

Spin glasses (SG's) are disordered magnetic alloys, widely regarded as paradigmatic complex systems.¹ The degree of anisotropy in the magnetic interactions determines whether a particular alloy is classified as a Heisenberg or an Ising SG (Ising corresponds to a limit of strong anisotropy). Experimentally, anisotropies affect significantly the glassy response to external magnetic fields and the behavior under cooling protocols.²

Theorists have privileged the study of the Ising limit, in spite of the fact that canonical SG's, e.g. CuMn or AgMn, should be rather regarded as Heisenberg, with weak anisotropic interactions. Indeed, complications arise in the Heisenberg case. In addition to the standard SG ordering, Heisenberg systems show as well a chiral-glass (CG) phase, where *chiralities* order³ (chiralities, also named vorticities, reflect the handedness of the non-collinear spin ordering pattern, see definitions below).

Probably motivated by failures in early numerical attempts⁴ to find a standard SG phase for Heisenberg systems, Kawamura proposed a *chirality scenario*, expected to hold for most experimental systems.⁵ In the ideal, fully isotropic case, the standard SG critical temperature T_{SG} would be strictly zero, while chiralities would order at $T_{CG} > 0$ (spin-chirality decoupling). Yet, anisotropic interactions (either dipolar, pseudo-dipolar or Dzyaloshinskii-Moriya^{6,7}), albeit small, are unavoidable in experimental samples. Hence, the scenario includes a *decoupling-recoupling* hypothesis: weak random anisotropic interactions would recouple spins and chiralities so that $T_{CG} = T_{SG} > 0$. Indeed, the numerical work available at the time indicated that very small amounts of anisotropy lead to $T_{SG} > 0$.⁸

CG ordering may be experimentally investigated through the anomalous Hall effect. Due to spin-orbit interaction and the spin polarization of the conduction electrons, the anomalous Hall resistivity picks contributions proportional to the CG order parameter and to its corresponding non-linear susceptibility.^{9,10} The effectiveness of this tool to study non-coplanar orderings has been

demonstrated in manganites,¹¹ and in a geometrically frustrated pyrochlore ferromagnet.¹²

The effect of anisotropies on the critical behavior was considered by Bray and Moore,⁷ before the question of chiral ordering was raised. They predicted that these systems belong to the Ising SG's Universality Class, no matter the kind of anisotropic interactions. However, in their analysis the assumption was made that $T_{SG} = 0$ in the isotropic limit (this assumption seemed plausible at the time, although we now know that it is incorrect).

Recent theoretical work has shown that the chirality scenario needs some revision. New simulation algorithms (allowing to thermalize at lower temperatures than pioneering work⁴), combined with modern finite-size scaling (FSS) methods,^{13–15} have provided conclusive evidence for a standard SG ordering with $T_{SG} > 0$ for purely isotropic interactions.^{16–22} Only some controversy remains on whether T_{SG} is slightly smaller than T_{CG} ,¹⁹ or rather the two are compatible within errors.²⁰ Interestingly enough, a modern-styled study seems to be still lacking for the more realistic case of a Heisenberg SG with small random anisotropy.

Here we show that small anisotropic interactions cause that, at variance with the ideal case, the CG susceptibility no longer diverges at T_{CG} (i.e. the anomalous dimension becomes $\eta_{CG} > 2$). In the Renormalization Group framework,¹⁵ anisotropy is a relevant perturbation. Even if in an experimental sample anisotropies are fairly small, the isotropic model is appropriate only for moderate correlation length. Closer to the critical temperature, a new fixed point rules (presumably in the Ising SG Universality Class, due to spin-reversal symmetry). A slow crossover¹⁵ from the Heisenberg to the anisotropic fixed-point arises upon approaching the phase transition. We conjecture that this crossover explains²³ experimental claims of a non-trivial dependency of critical exponents on the anisotropy strength.^{2,24} Our results follow from a FSS analysis of equilibrium Monte Carlo simulations on system-sizes up to $L = 32$. Data suggest that anisotropies cause a temperature range in which chiralities order while spins do not (i.e. $T_{SG} < T_{CG}$). However, due to the slow crossover, further research will be needed to dismiss spin-chirality recoupling.

The remaining part of this work is organized as follows. We define the model and describe our numerical methods in Sect. II. We address thermal equilibration, a major issue in any spin-glass simulation, in Sect. III. Our physical results are reported in Sect. IV. Finally, we give our results in Sect. V.

II. MODEL AND SIMULATIONS

Since the main types of anisotropic interactions lead to the *same* effective replica Hamiltonian,⁷ it is numerically convenient to study short range (pseudo-dipolar) interactions. Take the Edwards-Anderson model on a cubic lattice of size L , with periodic boundary conditions. Heisenberg spins occupy the lattice nodes \mathbf{x} [$\vec{S}_{\mathbf{x}} = (S_{\mathbf{x}}^1, S_{\mathbf{x}}^2, S_{\mathbf{x}}^3)$, $\vec{S}_{\mathbf{x}} \cdot \vec{S}_{\mathbf{x}} = 1$]. The Hamiltonian is⁸

$$H = - \sum_{\langle \mathbf{x}, \mathbf{y} \rangle} \left(J_{\mathbf{x}\mathbf{y}} \vec{S}_{\mathbf{x}} \cdot \vec{S}_{\mathbf{y}} + \vec{S}_{\mathbf{x}} \cdot D_{\mathbf{x}\mathbf{y}} \vec{S}_{\mathbf{y}} \right), \quad (1)$$

($\langle \mathbf{x}, \mathbf{y} \rangle$: lattice nearest-neighbors). The random exchange-couplings, $J_{\mathbf{x}\mathbf{y}}$, are Gaussian distributed with $\overline{J_{\mathbf{x},\mathbf{y}}} = 0$, and $\overline{J_{\mathbf{x},\mathbf{y}}^2} = 1$. The random $D_{\mathbf{x}\mathbf{y}}$ are 3×3 symmetric matrices (i.e. $\vec{S}_{\mathbf{x}} \cdot D_{\mathbf{x}\mathbf{y}} \vec{S}_{\mathbf{y}} = D_{\mathbf{y}\mathbf{x}} \vec{S}_{\mathbf{x}} \cdot \vec{S}_{\mathbf{y}}$). Their matrix elements are independent and uniformly distributed in $(-D, D)$. In most of the work reported here $D = 0.05$ (which corresponds to the best studied case⁸), but we will be presenting results for $D = 0.1$ as well.

The ideal limit of a fully isotropic Heisenberg model is recovered from Eq. (1) by setting $D = 0$. Once $D > 0$, the original O(3) symmetry, corresponding to a global spin rotation (or reflection), is lost. The only remaining symmetry for $D > 0$ is global spin inversion.

An instance of the couplings, $\{J_{\mathbf{x},\mathbf{y}}, D_{\mathbf{x},\mathbf{y}}^{\mu\nu}\}$ is named a *sample*. For any physical quantity, we first obtain the thermal average, denoted as $\langle \dots \rangle$. Only afterwards we perform the sample average (denoted by an overline).

Defining the SG and CG susceptibilities requires real replicas. We consider pairs of spin configurations, $\vec{S}_{\mathbf{x}}^a$ and $\vec{S}_{\mathbf{x}}^b$, that evolve with independent thermal noise, under the same couplings and at the same temperature. The spin-overlap field is $q_{\mathbf{x}} = \vec{S}_{\mathbf{x}}^a \cdot \vec{S}_{\mathbf{x}}^b$, while its Fourier transform at wave vector \mathbf{k} , is $\hat{q}_{SG}(\mathbf{k}) = \sum_{\mathbf{x}} q_{\mathbf{x}} e^{i\mathbf{k} \cdot \mathbf{x}} / N$. On the other hand, the local chirality is defined as:

$$\zeta_{\mathbf{x}\mu} = \vec{S}_{\mathbf{x}+\mathbf{e}_{\mu}} \cdot (\vec{S}_{\mathbf{x}} \times \vec{S}_{\mathbf{x}-\mathbf{e}_{\mu}}), \quad \mu = 1, 2, 3, \quad (2)$$

where \mathbf{e}_{μ} is the unit lattice vector along the μ axis. From (2), the chiral overlap-field is $\kappa_{\mathbf{x},\mu} = \zeta_{\mathbf{x},\mu}^a \zeta_{\mathbf{x},\mu}^b$, where the superindices a and b correspond to the replicas. Its Fourier transform is $\hat{q}_{CG}^{\mu}(\mathbf{k}) = \sum_{\mathbf{x}} \kappa_{\mathbf{x},\mu} e^{i\mathbf{k} \cdot \mathbf{x}} / N$.

The wave-vector dependent susceptibilities are:

$$\chi_{SG}(\mathbf{k}) = N \overline{\langle |\hat{q}_{SG}(\mathbf{k})|^2 \rangle}, \quad \chi_{CG}^{\mu}(\mathbf{k}) = N \overline{\langle |\hat{q}_{CG}^{\mu}(\mathbf{k})|^2 \rangle}. \quad (3)$$

$T \setminus L$	6	8	12	16	24	32
0.187	1000	1080	1000	1020	1000	1000
0.194	1000	1080	1000	1020	1000	—
0.200	1000	1080	1060	1020	1000	—
0.210	1000	1080	1000	1020	1200	1000
0.220	1000	1080	1000	1020	1080	—
0.230	1000	1080	1000	1020	1080	1000
0.240	1000	1080	1000	1020	1080	—
0.250	1000	1040	1000	1020	1000	—
EMCS $\times 10^5$	3	3	1.8	3.6	4.8	15

TABLE I: **Details of simulations with $D = 0.05$.** For each lattice size and temperature, we give the number of simulated samples. The last row indicates the number of Elementary Monte Carlo Steps (EMCS). The L -dependent EMCS consisted of 1 Heat-Bath full lattice sweep, followed by $5L/4$ sequential (microcanonical) overrelaxation sweeps. We took 6×10^4 measurements per sample, but for $L = 32$ (15×10^4 measurements).

$T \setminus L$	6	8	12	16
0.230	300	100	100	320
0.240	300	100	100	260
0.250	300	100	100	360
0.260	200	500	500	820
0.270	200	400	500	560
0.280	120	600	500	500
EMCS $\times 10^5$	3	3	1.8	3.6

TABLE II: As in Table I, for our simulations with $D = 0.1$.

The correlation length, either SG or CG, is^{15,25}

$$\xi = \frac{1}{2 \sin(k_{\min}/2)} \left(\frac{\chi(\mathbf{0})}{\chi(\mathbf{k}_{\min})} - 1 \right)^{1/2}, \quad (4)$$

where $\mathbf{k}_{\min} = (2\pi/L, 0, 0)$ or permutations.²⁶

Our simulation algorithm combines heat-bath with microcanonical overrelaxation.²⁷ Both moves generalize straightforwardly to the anisotropic case.²⁸ The mixed algorithm is effective for the isotropic Heisenberg SG^{17–20,29} and for other frustrated models.³⁰ Besides, we extrapolate to nearby temperatures using a bias-corrected³¹ data reweighting method.³² Most of our simulations were carried out with $D = 0.05$, see Table I. Nevertheless, we did as well some work for $D = 0.1$, see Table II.

III. EQUILIBRATION

We considered three thermalization tests. *First*, consider the identity (valid for Gaussian-distributed $J_{\mathbf{x},\mathbf{y}}$):

$$\Delta \equiv \frac{q_s - q_l}{T} + \frac{2}{z} U = 0, \quad (5)$$

where $U = - \sum_{\langle \mathbf{x}, \mathbf{y} \rangle} J_{\mathbf{x},\mathbf{y}} \langle \vec{S}_{\mathbf{x}} \cdot \vec{S}_{\mathbf{y}} \rangle / L^D$, the link-overlap is $q_l = 2 \sum_{\langle \mathbf{x}, \mathbf{y} \rangle} \langle \vec{S}_{\mathbf{x}}^a \cdot \vec{S}_{\mathbf{y}}^a \rangle \langle \vec{S}_{\mathbf{x}}^b \cdot \vec{S}_{\mathbf{y}}^b \rangle / (zL^D)$, while $q_s =$

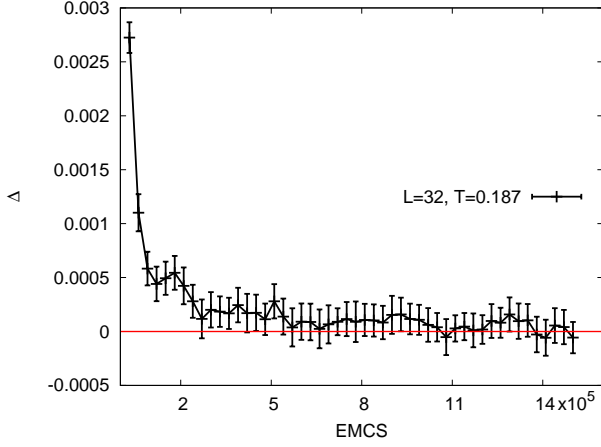


FIG. 1: (color online) Sample-averaged Δ defined in the l.h.s. of Eq. (5) vs. Monte Carlo time, as computed for $L = 32$ at $T = 0.187$ and $D = 0.05$. The EMCS was defined in the caption to Table I. Each point is an average over 3000 consecutive measurements.

$2 \sum_{\langle x, y \rangle} \langle (\vec{S}_x \cdot \vec{S}_y)^2 \rangle / (zL^D)$ ($z = 6$ is the lattice coordination number). Now, both U and q_s equilibrate easily. Yet, since q_l involves *two* replicas, it slowly grows from zero until its equilibrium value. Thus, a thermalization bias shows up as $\Delta > 0$.^{17,20,33} The time evolution of Δ , for $L = 32$ at the lowest T , is in Fig. 1. *Second*, we carried out the standard logarithmic data binning: we compare averages over the second half of the Monte Carlo history, with the second fourth, the second eight, and so forth, finding stability for three bins. *Third*, we checked for compatibility among reweighting extrapolations for contiguous temperatures (our simulations at different T are statistically independent, see Fig. 2).

IV. RESULTS

Our FSS analysis compares the correlation length in units of the lattice size for pairs of lattices $(L, 2L)$.^{13–15} Dimensionless quantities, such as ξ/L , are functions of $L^{1/\nu}(T - T_c)$, ν being the thermal critical exponent. Thus, the two curves intersect at $T_c(L, 2L)$, see Fig. 2. $T_c(L, 2L)$ differs from T_c due to scaling corrections (but tends to it for large L ¹⁵). Our dimensionless quantities ξ_{SG}/L and ξ_{CG}/L , produce two L -dependent critical temperatures $T_{SG}(L, 2L)$ and $T_{CG}(L, 2L)$. We compute the anomalous dimensions η from the scaling of the susceptibilities χ [take $\mathbf{k} = \mathbf{0}$ in Eq. (3)]. For large L , and $\eta < 2$, χ diverges as $\chi \propto |T - T_c|^{-\nu(2-\eta)}$. For finite L , we consider the susceptibility ratio for χ_{CG} and χ_{SG} (the dots stand for scaling corrections):

$$\left. \frac{\chi(2L)}{\chi(L)} \right|_{T_c(L, 2L)} = 2^{2-\eta} + \dots \quad (6)$$

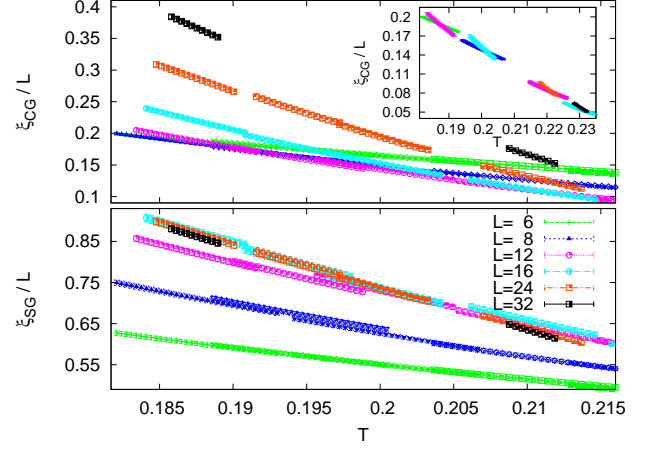


FIG. 2: (color online) Correlation length in units of the lattice size vs. T , for all our system sizes at $D = 0.05$. Results for both the CG (**top**), and the SG sectors (**bottom**). Data *patches* correspond each to an independent simulation (we used data reweighting³²). **Inset**: CG intersections for pairs of sizes $(L, 2L)$. The range of T and ξ_{CG}/L differ from main plot.

L	$T_{SG}(L, 2L)$	$T_{CG}(L, 2L)$	$2 - \eta_{SG}$	$2 - \eta_{CG}$
6	0.251(2)	0.187(1)	2.031(11)	0.360(8)
8	0.235(1)	0.202(1)	2.131(9)	0.223(8)
12	0.207(5)	0.221(1)	2.413(46)	0.081(5)
16	0.179(10)	0.233(1)	2.639(55)	0.030(5)

TABLE III: Size-dependent critical temperatures $T_{SG}(L, 2L)$ and $T_{CG}(L, 2L)$, and anomalous dimensions $2 - \eta_{SG}$ and $2 - \eta_{CG}$, Eq. (6), for the simulations with $D = 0.05$. Errors were obtained with jackknife.

We discuss first the CG sector. The inset of Fig. 2 shows an unusual feature: ξ_{CG}/L at the crossing point $T_{CG}(L, 2L)$ approaches zero for large L . This is to be expected only if $\eta \geq 2$:¹⁵ if the susceptibility does not diverge at T_c , the correlation length in Eq. (4) scales as $\xi/L \sim L^{-(\eta-2)/2}$. Nevertheless, we still find crossings when comparing lattices sizes L and $2L$, see Fig. 2 and also Ref. 34. Crossings are due to the fact that, in the large- L limit, the correlation length in Eq. (4) *is* divergent in the low-temperature phase. For $T < T_c$, ξ/L grows as $L^{\theta/2}$ (i.e. the correlation function at large distances r goes to a constant with corrections of order $1/r^\theta$, see e.g. Ref. 35). Yet, the susceptibility ratio in Eq. (6) is constant for large L , even if $\eta > 2$. So, η_{CG} in Table III approaches 2 as L grows.

Besides, it is note worthy that, in spite of the smallness of D , $T_{CG}(L, 2L)$ for $D = 0.05$ is about twice its value for the isotropic model, $T_{CG}(D = 0) \approx 0.13$.²⁰ In fact, extrapolating the data in Table III as $T_{CG}(L, 2L) = T_{CG} + A/L$ yields $T_{CG} \approx 0.26$.

To further investigate the lacking divergence of χ_{CG} at

T_{CG} , we consider the integrals³⁶

$$I_k = \sum_{r=0}^{L/2} r^k C_{P,P}(r), \quad (7)$$

where $C_{P,P}(r)$ is the plane-to-plane correlation function.³⁷ Note that $\chi_{CG} \sim 2I_0$, which means that plane-to-plane correlation functions decays with r slower than the standard point-to-point correlations by a factor r^{D-1} . The scaling behavior of the integrals (7) is: $I_k \sim \text{constant}$ in the paramagnetic phase, $I_k \sim L^{k+2-\eta}$ at T_{CG} (if $k+2-\eta > 0$, otherwise it is $I_k \sim \text{constant}$), and $I_k \sim L^{D+k}$ in the CG phase. We show in Fig. 3–top our data for χ_{CG} (which is basically $2I_0$) and, in Fig. 3–bottom, I_1 . Note that for $T < 0.22$ the two integrals are diverging with L . On the other hand, for $T = 0.22, 0.23$, I_1 grows with L , while χ_{CG} does not, as expected for $2 < \eta_{CG} < 3$.

The behavior of the SG sector is more conventional. A remarkable feature in Fig. 2 and Table III is the strong scaling corrections in $T_{SG}(L, 2L)$. We do not consider it safe to extrapolate T_{SG} to its large- L limit, as we are far from the asymptotic regime. The SG anomalous dimension takes a negative value as L grows (also found in the Ising SG, see e.g.¹³).

An intriguing feature is that T_{SG} seems smaller than T_{CG} . Indeed, see Fig. 2, at $T \approx 0.187$, where ξ_{SG}/L becomes L -independent, ξ_{CG}/L is growing fast with L . Yet, three caveats prevent us from considering this conclusion as definitive: (i) our lattice sizes are still in a strong cross-over regime, hence the final picture could change as L grows, (ii) the behavior is rather marginal, meaning a larger number of samples would be needed to accurately locate T_{SG} (this is hardly surprising, given the large value of exponent ν , and the small θ exponent, for $d = 3$ Ising SG's), and (iii) when considering a larger anisotropy, see below, the effect seems smaller.

Indeed, we have performed further simulations with $D = 0.1$, up to $L = 16$. As shown in Fig. 4, the difference between T_{SG} and T_{CG} is less clearly defined than for $D = 0.05$. On the other hand, the chiral-glass susceptibility is not divergent at the critical point, in agreement with our results for $D = 0.05$. Consistently with that, the crossing points for ξ_{CG}/L shift to a smaller height when L grows.

V. CONCLUSIONS

In summary, we have performed a finite size scaling study of the 3d Heisenberg spin glass in the presence of a weak random anisotropy, for lattices of size up to $L = 32$. Anisotropies cause that the CG susceptibility no longer diverges at T_{CG} , the chiralities ordering temperature. Hence, the anisotropic system belongs to a Universality Class different from the isotropic model (probably that of Ising SG's). Besides, we found that the spin-glass ordering sets up only at $T_{SG} < T_{CG}$. The most economic scenario is that actually $T_{SG} = T_{CG}$ (the

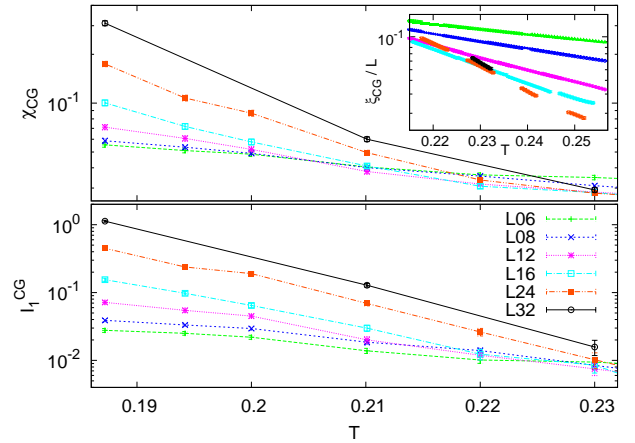


FIG. 3: Chiral glass susceptibility χ_{CG} (**top**) and I_1 integral defined in Eq. 7 (**bottom**) vs. temperature, for all our system sizes with $D = 0.05$. Lines are guides to eyes. **Inset**: zoom of ξ_{CG}/L vs. T

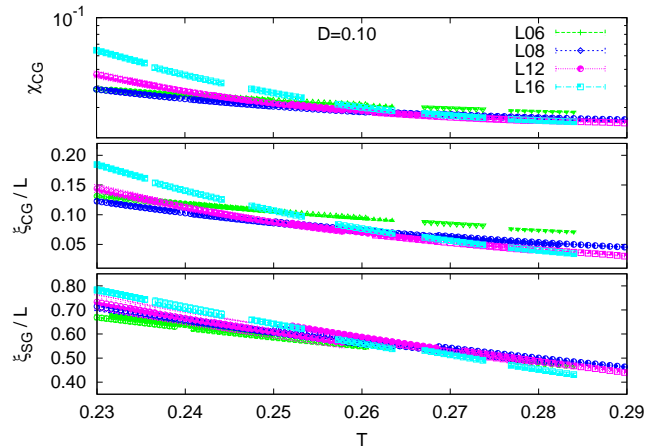


FIG. 4: For all our lattice sizes at $D = 0.1$, we show the chiral-glass susceptibility (**top**), as well as the CG (**center**) and SG (**bottom**) correlation lengths in units of the system size, as a function of temperature.

apparent difference would be due to finite-size effects). In this scenario, chiralities would merely be a composite operator (such as, say, the ninth power of the spin overlap). However, the would-be intermediate temperature region where only chiralities order should be experimentally detectable through the anomalous Hall effect. Numerical studies covering a wider range of values for the anisotropic coupling could also help to elucidate the situation.

ACKNOWLEDGMENTS

We thank A. Tarancon, G. Parisi and P. Young for discussions. Simulations were performed at BIFI (*Terminus*, 6.6×10^5 hours of CPU time) and Red Española

de Supercomputación (*Caesaraugusta*, 2.79×10^5 hours), whose staff we thank for the assistance provided. We were partly supported by MICINN (Spain) through research contract No. FIS2009-12648-C03, and (S.P.G.) through the FECYT Foundation.

-
- ¹ See e.g. *Spin Glasses and Random Fields*, Ed. A. P. Young. World Scientific (Singapore, 1997).
- ² F. Bert *et al.*, Phys. Rev. Lett. **92**, 167203 (2004).
- ³ A. Mauger *et al.*, Phys. Rev. B **41**, 4587 (1990).
- ⁴ W.L. McMillan, Phys. Rev. B **31**, 342 (1985); J.A. Olive, A.P. Young and D. Sherrington, *ibid* **34**, 6341 (1986); B.M. Morris *et al.*, J. Phys. C **19**, 1157 (1986).
- ⁵ H. Kawamura, Phys. Rev. Lett. **68**, 3785 (1992), *ibid* **80**, 5421 (1998).
- ⁶ P. M. Levy and A. Fert, Phys. Rev. B **23**, 4667 (1981).
- ⁷ A. J. Bray and M. A. Moore, J. Phys. C: Solid State Phys. **15**, 3897 (1982).
- ⁸ F. Matsubara, T. Iyota and S. Inawashiro, Phys. Rev. Lett. **67**, 1458 (1991).
- ⁹ G. Tataru and H. Kawamura, J. Phys. Soc. Jpn. **71**, 2613 (2002).
- ¹⁰ H. Kawamura, Phys. Rev. Lett. **90**, 047202 (2003).
- ¹¹ P. Matl *et al.*, Phys. Rev. B **57**, 10248 (1998); J. Ye *et al.*, Phys. Rev. Lett. **83**, 3737 (1999); S.H. Chun *et al.*, Phys. Rev. Lett. **84**, 757 (2000);
- ¹² Y. Taguchi *et al.*, Science **291**, 2573 (2001).
- ¹³ H. G. Ballesteros *et al.*, Phys. Rev. B **62**, 14237 (2000).
- ¹⁴ H. G. Ballesteros *et al.*, Phys. Lett. B **378**, 207 (1996); **B387**, 125 (1996), Nucl. Phys. B **483**, 707 (1997).
- ¹⁵ See, e.g., D. Amit and V. Martin-Mayor, *Field Theory, the Renormalization Group and Critical Phenomena*, (World-Scientific Singapore, third edition, 2005).
- ¹⁶ L.W. Lee and A.P. Young, Phys. Rev. Lett. **90**, 227203 (2003).
- ¹⁷ L.W. Lee and A.P. Young, Phys. Rev. B **76**, 024405 (2007).
- ¹⁸ I. Campos *et al.*, Phys. Rev. Lett. **97**, 217204 (2006).
- ¹⁹ D. X. Viet and H. Kawamura, Phys. Rev. Lett. **102**, 027202 (2009).
- ²⁰ L. A. Fernandez *et al.*, Phys. Rev. B **80**, 024422 (2009).
- ²¹ F. Matsubara, T. Shirakura and S. Endoh, Phys. Rev. B **64**, 092412 (2001); T. Nakamura and S. Endoh, J. Phys. Soc. Jpn. **71**, 2113 (2002).
- ²² F. Matsubara, T. Shirakura, S. Endoh and S. Takahashi, J. Phys. A: Math. Gen **36**, 10881 (2003).
- ²³ The quasi long-ranged Dzyaloshinskii-Moriya interactions induce an additional crossover, from mean-field to three-dimensional behavior.⁷
- ²⁴ I. A. Campbell, and D. Petit, J. Phys. Soc. Jpn. **79**, 011006 (2010).
- ²⁵ F. Cooper, B. Freedman and D. Preston, Nucl. Phys. B **210**, 210 (1982).
- ²⁶ We will not make any distinction between the CG longitudinal or transversal correlation lengths, see e.g. Ref. 16, since the two turn out to be compatible within errors.
- ²⁷ F. R. Brown and T. J. Woch, Phys. Rev. Lett. **58**, 2394 (1987).
- ²⁸ Eq. (1) can be split as $H = \vec{h}_x \cdot \vec{S}_x + H'$; H' is independent of \vec{S}_x , while $\vec{h}_x = \sum_{\|x-y\|=1} [J_{x,y} \vec{S}_y + D_{x,y} \vec{S}_y]$.
- ²⁹ J. H. Pixley and A. P. Young, Phys. Rev. B **78**, 014419 (2008).
- ³⁰ J. L. Alonso *et al.*, Phys. Rev. B **53**, 2537 (1996); E. Marinari, V. Martin-Mayor and A. Pagnani, *ibid* **62** (2000) 4999.
- ³¹ H. G. Ballesteros *et al.*, Nucl. Phys. B **512**, 681 (1998).
- ³² M. Falcioni *et al.*, Phys. Lett. B **108**, 331 (1982); A. M. Ferrenberg and R. H. Swendsen, Phys. Rev. Lett. **61**, 2635 (1988).
- ³³ H. G. Katzgraber, M. Palassini and A. P. Young, Phys. Rev. B, **63**, 184422 (2001).
- ³⁴ J.L. Alonso *et al.*, Phys. Rev. B **71**, 014420 (2005).
- ³⁵ R. Alvarez-Baños *et al.* (Janus Collaboration), Phys. Rev. Lett. **105**, 177202 (2010) and J. Stat. Mech. (2010) P06026.
- ³⁶ F. Belletti *et al.* (Janus Collaboration), Phys. Rev. Lett. **101**, 157201 (2008).
- ³⁷ For planes parallel to (say) the $\mu=3$ lattice axis, add the correlation function for all pairs of sites $\mathbf{x} = (n_1, n_2, n_3)$, $\mathbf{y} = (m_1, m_2, m_3)$ such that $m_3 - n_3 = r + kL$, with k integer, then divide by L^D . We average over the three lattice directions, as well as over the longitudinal (weight 1/3) and the transversal (weight 2/3) correlation functions.